

ADVANCEMENTS IN INJECTION EFFICIENCY MODELLING FOR THE LOW ENERGY ION RING (LEIR) AT CERN

R. Alemany Fernandez, G. Bellodi, N. Biancacci, D. Bodart, M. Bozzolan, N. Madysa, P. D. Meruga, R. Scrivens, CERN, Geneva, Switzerland

Abstract

The performance of the Low Energy Ion Ring (LEIR) at CERN is mainly determined by the number of charges extracted from the machine and transferred to the downstream chain of accelerators. While the required target of 9×10^{10} charges has now been surpassed, a series of studies have been undertaken to further push the intensity reach of LEIR. In this work, we quantify the effect of the stray fields generated by the adjoining Proton Synchrotron (PS), which were recently partially shielded, and the effect of the stripper foil in the Linac supplying LEIR with its ions, Linac 3. The impact of the stray field was measured by observing the variation in injection trajectory, while that of the stripper foil was determined from the evolution of the Schottky energy profile in LEIR. Models have been developed to extrapolate the impact of these effects to the injection efficiency of LEIR, and consequently to the extracted beam intensity.

INTRODUCTION

In 2022, the LEIR machine provided Pb ions to the fixed target experiments and the LHC. Following the performance improvements made in the last years [1, 2], a significant effort was recently put into the improvement of the machine reproducibility identifying the effects affecting the accelerator performance over time. The most important sources identified so far are the stray fields from the PS, and the evolution of the stripper foil performance. In this work, we will discuss the measurements performed to quantify both effects and the measures taken to mitigate them. We will also describe a tracking tool developed for the calculation of the LEIR injection efficiency under the influence of these effects.

STRAY FIELDS FROM THE PS

The Pb beam produced by the Linac 3, is transported through the lines ITH, ITE, ETL and EI to reach the LEIR injection region. Among these, part of the ITE line is physically close to the PS main dipoles. The first magnetic measurements of the PS stray field disturbance in the ITE lines are summarised in [3], as well as computations of the kick that the Pb beam would experience on its trajectory to LEIR. A shielding campaign took place during the shutdown period between 2021 and 2022. Figure 1 shows the installed shields in ITE and the proximity of the PS main bends. The installed panels consist of steel plates spaced by sheets of epoxy loaded fiberglass laminates. Each panel is securely mounted to avoid movement due to the magnetic forces: it is positioned on a fixture and slides vertically by hand, while fasteners ensure a proper tightening of the assembly.



Figure 1: Part of the ITE line from Linac 3 to LEIR. Magnetic shields have been installed to reduce the stray fields from the close-by PS main bend. Beam travels from left to right.

In the present configuration, a reduction of a factor 2 to 3 in stray field magnitude is expected [4]. The recently installed beam position monitors (BPMs) between the ITE and EI lines, allowed accurate beam trajectory measurements to be performed that were compared to 2021, when no shielding was present. Figure 2 shows the displacement in trajectory that the beam experiences when the PS main bends reach a magnetic field above 12 kG. The reference trajectory is relative to a PS magnetic field below 5 kG, a range in which no relevant perturbation is induced. We observe a reduction in the slope after the shielded region, especially in the V plane, compatible with a factor 2 reduction in stray field effect. Nevertheless, the displacement collected along the line is still large and visible already before the shielded region: this could point to additional un-shielded locations in the remaining part of the ITE loop and will be subject of future investigation and measurements.

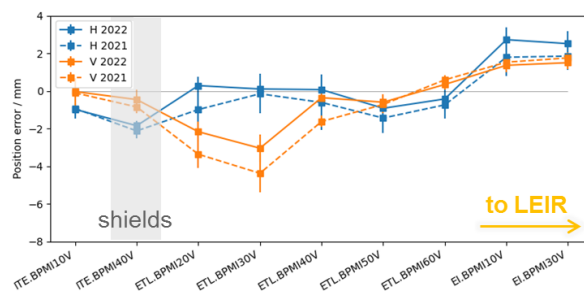


Figure 2: Trajectory displacement measured with the BPM system installed in ITE, ETL and EI lines.

STRIPPER FOIL EVOLUTION

Stripper foils are installed at the end of the accelerating stages of Linac 3, with the aim of stripping Pb²⁹⁺ to Pb⁵⁴⁺

for LEIR. This process is nevertheless slowly degrading the stripping performance and as a consequence, the intensity achievable in the downstream machines [5]. Recent improvements in the foils have dramatically increased the reproducibility of the performance between new foils. Thanks to this it has been possible to observe the performance variation during their life cycle.

In 2021, Schottky measurements were performed and new simulation tools developed to characterise the beam energy distribution produced by Linac 3 [6] as a function of the stripper foil thickness, ramping cavity (RC) and debunching cavity (DC) settings [2]. In particular, the start/end phases of the RC and DC could be varied in order to change the beam energy distribution delivered to LEIR and/or to compensate for the evolution of the stripper foil performance.

This activity continued in 2022, from both the Linac 3 and LEIR sides, with the aim of better monitoring the stripper foil performance evolution and predicting the moment in which the foil should be changed for a new one.

Figure 3 shows the mean and standard deviation of the momentum spread measured for different foils of similar density by taking the beam into the ITFS measurement line onto a secondary emission monitor grid (see complete procedure in [5]): one can observe a significant drift versus time on both quantities. As in 2021, the foil was typically exchanged when the standard deviation σ_p/p reached a value close to 2×10^{-3} .

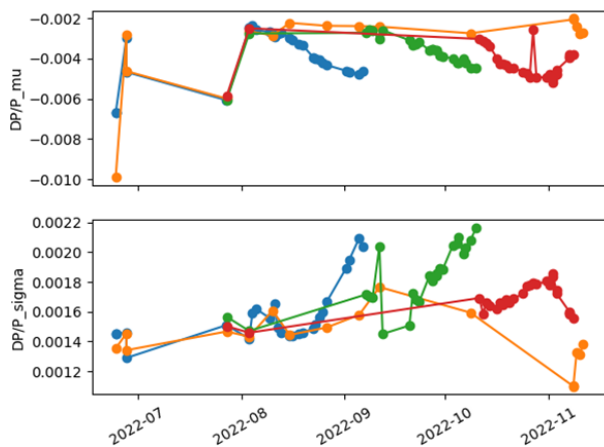


Figure 3: Evolution of the mean and standard deviation of the beam momentum measured after the Linac 3 ramping cavity. Different colors refer to different stripper foils.

An equivalent measurement was investigated in LEIR, in order to complement and strengthen the stripper foil monitoring tools and promptly identify and react to their performance evolution. Figure 4 shows the energy distribution measured in LEIR for a “mono-energetic” beam from Linac 3 achieved with equal start/end RC/DC phase of 20° . One can see how the low energy tail of the distribution increases over 2 weeks, showing the evolution in performance of the $127\mu\text{g}/\text{cm}^2$ stripper foil installed before the beginning of the measurements.

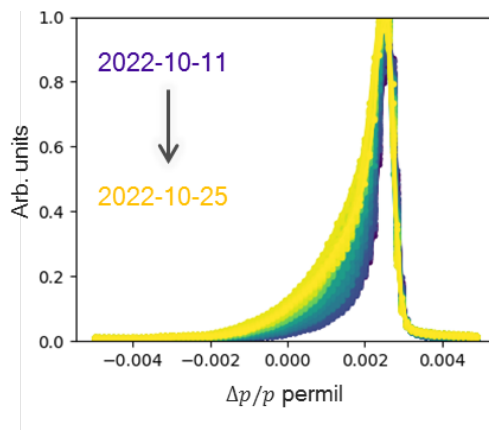


Figure 4: Energy distribution measured in LEIR with equal start/end RC and DC phase of 20° . Measurements over 2 weeks are shown in gradient color from purple to yellow.

INJECTION EFFICIENCY MODEL

Both the stray fields and the stripper foil performance evolution impact the injection efficiency in LEIR, which requires a careful adjustment of the incoming beam energy distribution and the transverse position at the electrostatic septum [7]. In the past, illustrative simulations were set up in [8] to show the injection process. Along this line, a new tracking tool was developed to quantitatively study the dependency of the injection efficiency on the aforementioned effects. The model is a branch of PyHEADTAIL [9], expanded in the last few years in order to study coasting beam collective effects driven by electron cooling, space charge, IBS and impedance [10], and their impact on Schottky spectra [11] in LEIR. The beam is modeled accounting for the energy distribution computed with [6] and tracked with a one-turn-map accounting for the machine acceptance and aperture model available on the optics repository [12].

Figure 5 shows the injection efficiency computed from tracking simulations and compared to measurements taken for different DC flat phases. The agreement is acceptable and within an absolute error of 5% in injection efficiency.

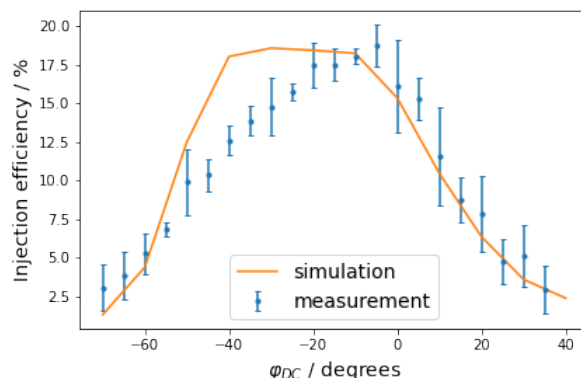


Figure 5: Measured and simulated injection efficiency as a function of the DC phase.

The injection process requires stacking of the Linac 3 beam over 70 turns [7]. Presently, due to the 10% longer beam from Linac 3, the process occurs in 80 turns, during which the intensity is accumulated in the ring and measured using a fast beam current transformer. Figure 6 shows the accumulated intensity versus turns for selected DC flat phases and for the operational case with DC ramped between -50° and 20° . The agreement is very good and inline with the one shown in Fig. 5.

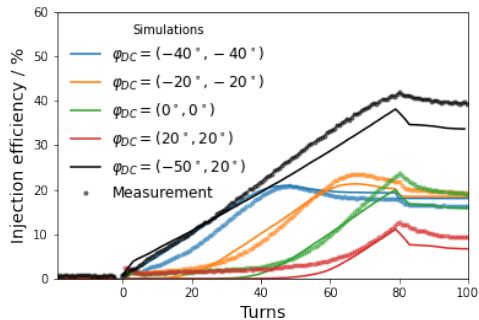


Figure 6: Measured and simulated intensity during the accumulation process in LEIR. The cases of flat and ramped DC phases are respectively shown in colors and in black. In parenthesis, the start/end phases of the DC are indicated.

The tool has also been used to study the loss in injection efficiency due to stray fields or stripper foil performance evolution. To model the stray field effect we apply a transverse displacement at the injection septum between 0 and 3 mm (i.e. extrapolated from the EI BPMs of Fig. 2). Figure 7 shows the loss in injection efficiency measured and predicted by applying the displacement either in H or H and V. This shows that in order to improve the machine stability the displacement should be less than 0.5 mm to limit to 5% the loss in injection efficiency and therefore preserve the target output intensity.

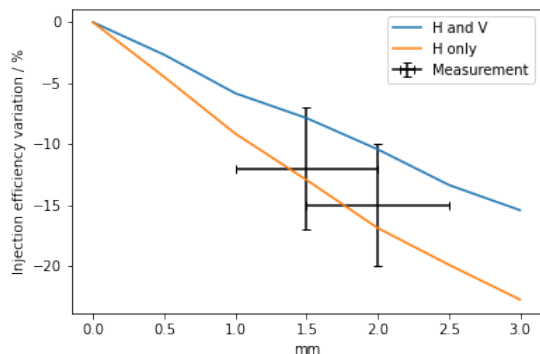


Figure 7: Relative loss in injection efficiency due to stray field effects.

The effect of the stripper foil evolution is modeled assuming a skew normal momentum distribution [13] with constant skewness $\alpha = -2$ and variable spread produced

after the stripper foil. Figure 8 shows the variation in injection efficiency when developing the low energy tail of Fig. 4 measured by the LEIR Schottky system. The agreement to the model is acceptable and we conclude that the momentum spread should have a standard deviation less than 1.45×10^{-3} to maintain the loss in injection efficiency below 5%. The measurements complement the one performed in ITFS (Fig. 3).

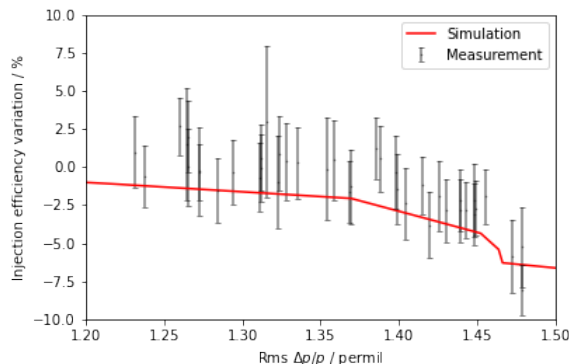


Figure 8: Relative loss in injection efficiency due to stripper foil performance evolution.

CONCLUSIONS

In this work we presented the advancements in the injection efficiency modelling and the improved understanding of the main mechanisms affecting the LEIR injection performance: the PS stray fields and the stripper foil evolution.

Concerning the stray fields, we showed the effect of magnetic shielding put in place in the ITE line: while a local reduction is visible, this is still not enough to suppress the impact on LEIR and further measures are envisaged.

Concerning the stripper foil performance, ad-hoc monitoring has been put in place in LEIR, complementary to the measurements done in the ITFS line: with careful adjustments of the RC and DC settings, the development of a low energy tail has been observed and correlated to the stripper foil performance evolution.

Based on these observations, a tracking tool has been developed to simulate the injection efficiency process of LEIR under the effect of stray fields and different energy profiles. The tool has been successfully benchmarked against the measurements in LEIR during the injection process. The impact of stray fields and low energy tail is modeled and in good agreement with measurements.

In order to maintain the variation of injection efficiency in LEIR below 5%, based on the tracking simulations, the stray field effect should be limited to 0.5 mm and the spread of the low energy tailed distribution should have a standard deviation less than 1.45×10^{-3} . A larger spread should trigger the foil exchange. A similar criterion has been developed when measuring the energy spread from the ITFS line.

REFERENCES

- [1] S. Albright *et al.*, “Review of LEIR operation in 2018”, CERN, Geneva, Switzerland, Rep. CERN-ACC-NOTE-2020-00231, Dec. 2019. <https://cds.cern.ch/record/2715365>
- [2] N. Biancacci, S. Albright, R. Alemany-Fernández, D. Alves, M.E. Angoletta, D. Barrientos, *et al.*, “Linac3, LEIR and PS Performance with Ions in 2021 and Prospects for 2022”, in *Proc. IPAC’22*, Bangkok, Thailand, Jun. 2022, pp. 1983–1986. doi:10.18429/JACoW-IPAC2022-WEPOPT055
- [3] N. Biancacci, D. Bodart and R. Alemany Fernandez, “Installation of a Shield for Stray Field Compensation Along the ITE and ETL Transfer Lines”, EDMS document n. 2659881 v.0.1, CERN, Geneva, Switzerland, 2020. <https://edms.cern.ch/document/2659881/0.1>
- [4] D. Bodart, “Stray field measurements after ITE line shielding”, in *LIU-Ions MPC meeting*, CERN, Geneva, Switzerland, 8 March 2022. <https://indico.cern.ch/event/1134997/>
- [5] G. Bellodi *et al.*, “Stripper foil investigations at Linac3”, CERN, Geneva, Switzerland, Rep. CERN-ACC-NOTE-2020-0016, Mar. 2020, <https://cds.cern.ch/record/2713678>
- [6] R. Scrivens, “Linac3 ramping tracking code”, GitLab repository, 2022, https://gitlab.cern.ch/scrivens/linac3_ramping
- [7] O. Brüning *et al.*, “LHC Design Report, Vol. III, The LHC Injector Chain”, CERN Yellow Reports, Switzerland, doi:10.5170/CERN-2004-003-V-1, 2004.
- [8] A. Huschauer, “Preparing LEIR for the HL-LHC Era”, BE Seminar, CERN, Geneva, Switzerland, Jun. 2017, <https://indico.cern.ch/event/639584>.
- [9] K. Li *et al.*, “PyHEADTAIL”, Github repository, <https://github.com/PyCOMPLETE/PyHEADTAIL>
- [10] N. Biancacci *et al.*, “LEIR Impedance Model and Coherent Beam Instability Observations”, in *Proc. IPAC’17*, Copenhagen, Denmark, May 2017, pp. 3159–3162. doi:10.18429/JACoW-IPAC2017-WEPIK094
- [11] N. Biancacci, “Interpretation of the LEiR Schottky spectra”, in *ABP-CEI meeting*, CERN, Geneva, Switzerland, 30 June 2022. <https://indico.cern.ch/event/1134997/>
- [12] “Low Energy Ion Ring Optics Repository”, 2022, <https://acc-models.web.cern.ch/acc-models/leir/>
- [13] Skew normal distribution, Wikipedia, https://en.wikipedia.org/wiki/Skew_normal_distribution